

ADVANCED SIMULATION OF TRANSIENT MULTIPHASE FLOW & FLOW ASSURANCE IN THE OIL & GAS INDUSTRY

Djamel Lakehal^{1,2*}

1. ASCOMP GmbH Zurich, Zurich, Switzerland

2. ASCOMP Inc., Cambridge, Massachusetts

We discuss here current computational trends (beyond Mechanistic 1D Models) related to transient multiphase flow and flow assurance problems in the oil and gas sector. The developments needed to bring advanced Computational fluid & *Multiphase*-fluid dynamics (CFD & CMFD) techniques and models to a mature stage will also be discussed. The contribution presents the possibilities offered today by these simulation technologies to treat complex, multiphase, multicomponent flow problems occurring in the gas and petroleum engineering in general. Examples of various degrees of sophistication will be presented, without focusing on the validation aspect as such. The models are briefly introduced (phase averages, N-phase, interface tracking, Lagrangian particle tracking and granular flow model).

Keywords: CFD, CMFD, multiphase, N-phase, turbulence

INTRODUCTION

Multiphase flows appear in various industrial processes and in the petroleum industry in particular, where oil, gas and water are often produced and transported together.^[1] During co-current flow in a pipe the multiphase flow topology can acquire a variety of characteristic distributions called flow regimes, or flow patterns, each featuring specific hydrodynamic characteristics (e.g. bubbly, slug, annular, mist, churn), depending on the phasic volumetric flow rates. In addition, the relative volumetric fraction of the phases can change along the pipes either because of heat addition from outside, heat exchanges between the phases or flashing due to depressurisation. Some of these hydrodynamic features are clearly undesirable particularly in the hydrocarbon transportation systems, for example slug flow, which may be harmful to some operations components. Such multiphase flows exist in oil and gas pipes to and from the reservoir, too. Indeed, in extraction and injection processes of oil and gas to and from reservoirs, multiphase mixtures of oil, natural gas and water (and also CO₂ in Carbon capture and sequestration, CCS and enhanced oil recovery, EOR) is piped between the reservoir and the surface. A good knowledge of the fluid mechanics in general and flow distribution there should have a significant impact on the well productivity (in EOR), well storage capacity (in CCS), production costs and equipment size. Further, new possibilities and challenges for advanced computational multiphase flow (called CMFD) are offered today in flow assurance where various complex issues—in particular as to the transport—appear and need to be addressed.

The complexity of multiphase flows in pipes increases with the presence of solid particles, including sand and black powder in gas pipelines. Particle-induced corrosion in oil and gas pipelines made from carbon steel occurs often, which requires the removal of pipe segments affected incurring extra costs and break in the distribution. To this we can add the catalytic reaction between the fluids and the pipe internal walls, including electrochemistry and water chemistry.^[2] Black powder deposition may lead to the formation of particle slugs in the pipes that can also be harmful to the operations. Further complexities may appear when phase change between the fluids occurs like the formation of hydrates from

methane and light components of oil, which could be remedied through the injection of additives like methanol or hot water.

For all these phenomena, high-fidelity predictive CFD/CMFD methods are sought to be applied in connection with laboratory experiments and prepare for safety prevention systems. This is true for flow assurance modelling, in particular as to subsea oil production and transport, and in other enhanced oil recovery systems, including using steam or Carbon Dioxide injection in wellbores. At the downstream level, say when use is made of the treated gas for energy production, various technical issues still pertain, as in the gas turbine combustion sector, where advanced CFD is also required to optimise the fuel injection, atomisation and mixing processes.

COMPUTATIONAL MULTIPHASE FLOW

Computational multiphase flow for various industrial sectors (e.g. process and chemical engineering and thermal hydraulics of nuclear reactors in particular) has gone through successive transitions, motivated by new possibilities, needs and developments. The first real transition triggered in the 1980s focused on gradually removing the limitations of lumped-parameter 1D modelling by further developing the two-fluid model for 3D turbulent flow problems. This is now the state-of-the-art. The advent of the so-called Interface Tracking Methods (ITM) in the late 1980s, which permit to better predict the shape of interfaces while minimising the modelling assumptions for momentum interaction mechanisms, has somewhat shifted the interest towards a new transition. The most recent transition is now underway: it specifically centres on the use of these new simulation techniques (ITM) for practical cases. But this latest transition poses interesting challenges and raises specific questions: how to migrate from averaged two-fluid

*Author to whom correspondence may be addressed.

E-mail address: lakehal@ascomp.ch

Can. J. Chem. Eng. 9999:1–14, 2013

© 2013 Canadian Society for Chemical Engineering

DOI 10.1002/cjce.21828

Published online in Wiley Online Library

(wileyonlinelibrary.com).

formulation modelling to more refined interface tracking prediction (or combine them when necessary, and from steady-state Reynolds averaged modelling to unsteady large-scale turbulence simulation. The transition is not a matter of availability of computational power and resources only, but a question of adequacy of code algorithmic, complex meshing and proper modelling of the underlying flow physics. The transition issue is well discussed by Lakehal^[3] though for another industrial context, but for which the same modelling and simulations techniques and models apply. The oil and gas sector has not really been the subject to any of these transitions; the iron-cast consensus is to use 1D Mechanistic Model codes^[4,5] like OLGA or LedaFlow.^[6] This is understandable when it comes to slug flow prediction in a 100 miles oil pipeline, certainly not for local component scale fluid dynamics, where the modelling accuracy is highly questionable due to the myriad of model uncertainties introduced by averaging, a part from the uncertainties brought by the experimental correlations.

Our objective here is to portray the large picture of multiphase flow in the gas and petroleum engineering, and introduce the state of the art in treating these using advanced CFD and CMFD, which could plan an important role besides 1D mechanistic models. The examples selected are prototypes only, selected for their specific physical complexity. While flow assurance engineers are used to 1D system codes we aim with this note to draw the attention to other ongoing parallel efforts, be they more expensive in terms of computational resources, and to the needs of completing (e.g. using 3D codes to infer closure models for 1D codes) or coupling these system codes with CFD/CMFD. Greatly improved predictive capabilities for multiphase flow and heat transfer are today offered by CMFD, in particular through the use of Interface Tracking Methods (ITM), which minimise the modelling efforts. The physical complexity of multiphase flows in hydrocarbon transportation and extraction naturally lends itself to such approaches.

MULTIPHASE FLOW MODELLING IN THE CODE TransAT

Multiphase-flow Code TransAT©

TransAT© is a finite-volume solver for single and multifluid Navier–Stokes equations on structured multi-block meshes, under collocated grid arrangement. The solver is Projection Type based, corrected using the Karki–Patankar technique for compressible flows. High-order time and convection schemes can be employed; up to 3rd-order Monotone and TVD-bounded schemes in space and 5th-order RK in time. An algebraic multigrid algorithm is employed for the pressure equation, involving relaxation, restriction and prolongation to achieve high rates of convergence. Multiphase flows can be tackled using either (i) interface tracking techniques (Level Set, Volume-Of-Fluid with 3rd-order interface reconstruction, and Phase Field), (ii) N-phase, phase-averaged mixture with Algebraic Slip or (iii) Lagrangian particle tracking (one-to-four way coupling). Besides Body-Fitted Coordinates (BFC) meshing capabilities, TransAT also uses the Immersed Surfaces Technique (IST) to map complex geometries into a rectangular Cartesian grid. Near-wall regions are treated with Block Mesh Refinement (BMR), a sort of geometrical multi-grid approach in which refined grid blocks or manifolds are placed around solids where adequate. This is different from the algebraic multigrid algorithm discussed above, in that each BMR block is separately solved and the solutions are passed from one block to the next as an initial flow field. The connectivity between blocks can be achieved in parallel up to 8-to-1 cell mapping.

The combination IST/BMR saves up to 70% grid cells in selected 3D problems and allows solving conjugate heat transfer and rigid-body motion problems.

Phase Average Models (Homogeneous Algebraic Slip Approach)

In the Homogeneous Algebraic Slip model^[7] applied to gas–liquid systems, the transport equations are solved for the mixture quantities (subscript m) rather than for the phase-specific quantities (subscripts G and L):

$$\mathbf{u}_m = \sum_{k=G,L} \frac{\alpha_k \rho_k \mathbf{u}_k}{\rho_m}; \quad \rho_m = \sum_{k=G,L} \alpha_k \rho_k \quad (1)$$

$$Y_k = \frac{\alpha_k \rho_k}{\rho_m}; \quad \mathbf{u}_D = \mathbf{u}_G - \mathbf{u}_m$$

where \mathbf{u} , ρ , α , Y and \mathbf{u}_D are the velocity, density, volume fraction, mass fraction and slip velocity, respectively. This implies that one mixture momentum equation is solved for the entire flow system, reducing the number of equations to be solved in comparison to the two-fluid model:

$$\partial_t \rho_m + \nabla \cdot (\rho_m \mathbf{u}_m) = 0 \quad (2)$$

$$\partial_t (\rho_G \alpha_G) + \nabla \cdot (\rho_G \alpha_G (\mathbf{u}_m + \mathbf{u}_D)) = 0 \quad (3)$$

$$\begin{aligned} \partial_t (\rho_m \mathbf{u}_m) + \nabla \cdot \rho_m \left(\mathbf{u}_m \mathbf{u}_m + \frac{Y_G}{Y_L} \mathbf{u}_D \mathbf{u}_D - \prod_m \right) \\ = \nabla \cdot [2\alpha_G \mu_G \boldsymbol{\sigma}_G^D + 2\alpha_L \mu_L \boldsymbol{\sigma}_L^D] + \rho_m g \end{aligned} \quad (4)$$

Closure models are required for the slip velocity (\mathbf{u}_D) and associated stresses $\overline{\mathbf{u}_D \mathbf{u}_D}$. The simplest model used for the slip velocity reads (for bubbly flows):

$$\mathbf{u}_D = \frac{2}{9} \frac{\alpha_L R_b^2 (\rho_G - \rho_L)}{\alpha_G \mu_m} Y_L (Y_L - \alpha_L) \nabla p \quad (5)$$

Phase Average Models (The N-Phase Approach)

The N-phase approach is invoked in situations involving more than two phases, for example gas–water–oil–hydrate, with the oil phase comprising both light and heavy components. The N-phase approach could as well be used in the two-fluid flow context. In the Homogeneous Algebraic Slip framework, the above transport Equations (2) and (3) become:

$$\partial_t (\rho_G \alpha_G) + \nabla \cdot (\rho_G \alpha_G (\mathbf{u}_m + \mathbf{u}_k^D)) = 0 \quad (6)$$

$$\begin{aligned} \partial_t (\rho_m \mathbf{u}_m) + \nabla \cdot \rho_m \left(\mathbf{u}_m \mathbf{u}_m + \sum_k Y_k \overline{\mathbf{u}_k^D \mathbf{u}_k^D} - \prod_m \right) \\ = \nabla \cdot \left(\sum_k 2\alpha_k \mu_k \boldsymbol{\sigma}_k^D \right) + \rho_m g \end{aligned} \quad (7)$$

with the drift velocity of each phase k given by $\mathbf{u}_k^D = \mathbf{u}_k \mathbf{u}_m$.

Interface Tracking Methods for Interfacial Flow

Interfacial flows refer to multi-phase flow systems that involve two or more immiscible fluids separated by sharp interfaces which evolve in space and time. Typically, when the fluid on one side of the interface is a gas that exerts shear (tangential) stress upon

the interface, the latter is referred to as a free surface. ITMs are best suited for these flows, because they represent the interface topology rather accurately, and are generally built within the so-called single-fluid formalism.^[8]

The single-fluid formalism solves a set of conservation equations with variable material properties and surface forces.^[8] The strategy is thus more accurate than the phase-average models as it minimises modelling assumptions. The incompressible multifluid flow equations within the single-fluid formalism read:

$$\nabla \cdot \mathbf{u} = 0 \quad (8)$$

$$\partial_t(\rho\mathbf{u}) + \nabla \cdot (\rho\mathbf{u}\mathbf{u}) = -\nabla p + \nabla \cdot \boldsymbol{\tau} + \mathbf{F}_s + \mathbf{F}_g \quad (9)$$

$$\mathbf{F}_s = \gamma\kappa\mathbf{n}\delta(\phi) + (\nabla_s\gamma)\delta(\phi) \quad (10)$$

where ρ is the density, p is the pressure, μ is the viscosity and $\boldsymbol{\tau}$ is the Cauchy stress. \mathbf{F}_g is the gravitational force, \mathbf{F}_s is the surface tension force, with \mathbf{n} standing for the normal vector to the interface, κ for the surface curvature, γ for the surface tension coefficient of the fluids, ∇_s for the surface gradient and δ for a smoothed Dirac delta function centred at the interface. In the Level Set technique^[9] the interface between immiscible fluids is represented by a continuous function ϕ , denoting the distance to the interface that is set to zero on the interface, is positive on one side and negative on the other. Material properties, body and surface forces are locally updated as a function of ϕ , and smoothed across the interface using a smooth Heaviside function:

$$\rho, \mu = \rho, \mu|_L \cdot H(\phi) + \rho, \mu|_G \cdot (1 - H(\phi)) \quad (11)$$

$$\partial_t\phi + \mathbf{u} \cdot \nabla\phi = 0 \quad (12)$$

In practice, the level set function ceases to be the signed distance from the interface after a single advection step of Eq. (12). To restore its correct distribution near the interface, a re-distancing equation is advected to steady state, using 3rd- or 5th order WENO schemes; more details can be found in Ref.^[8]

Lagrangian Particle Tracking

The Eulerian–Lagrangian formulation applies to particle-laden (non-resolved component entities) flows, under one-way, two-way or four-way coupling (also known as dense particle flow systems). Individual particles are tracked in a Lagrangian way in contrast to the former two approaches, where the flow is solved in the Eulerian manner, on a fixed grid. One-way coupling refers to particles cloud not affecting the carrier phase, because the field is dilute, in contrast to the two-way coupling, where the flow and turbulence are affected by the presence of particles. The four-way coupling refers to dense particle systems with mild-to-high particle volume fractions ($\alpha_p > 5\%$), where the particles interact with each other.

In the one- and two-way coupling cases, the carrier phase is solved in the Eulerian way, that is solving for the continuity and momentum equations:

$$\nabla \cdot \mathbf{u} = 0 \quad (13)$$

$$\partial_t(\rho\mathbf{u}) + \nabla \cdot (\rho\mathbf{u}\mathbf{u}) = -\nabla p + \nabla \cdot \boldsymbol{\tau} + \mathbf{F}_b + \mathbf{F}_{ip} \quad (14)$$

This set of transport equations is then combined with the Lagrangian particle equation of motion:

$$d_t(v_{pi}) = -(1 + 0.15Re_p^{2/3}) \frac{9\mu}{2\rho_p d_p^2} (\mathbf{u}_{pi} - \mathbf{u}_i[\mathbf{x}_{pi}(t)]) + \mathbf{g} \quad (15)$$

where \mathbf{u} is the velocity of the carrier phase, \mathbf{u}_{pi} is the velocity of the carrier phase at the particle location \mathbf{x}_{pi} , \mathbf{v}_{pi} is the particle velocity, $\boldsymbol{\tau}$ is the viscous stress and p is the pressure. The source terms in Equation (14) denote body forces, \mathbf{F}_b , and the rate of momentum exchange per volume between the fluid and particle phases, \mathbf{F}_{ip} . The coupling between the fluid and the particles is achieved by projecting the force acting on each particle onto the flow grid:

$$\mathbf{F}_{ip} = \sum_{i=1}^{N_p} \frac{\rho_p V_p}{\rho_m V_m} R_{rc} f_i W(\mathbf{x}_i, \mathbf{x}_m) \quad (16)$$

where i stands for the particle index, N_p for the total number of particles in the flow, f_i for the force acting on a single particle centered at \mathbf{x}_i , R_{rc} for the ratio between the actual number of particles in the flow and the number of computational particles, and W for the projection weight of the force onto the grid node \mathbf{x}_m , which is calculated based on the distance of the particle from those nodes to which the particle force is attributed. V_m is the fluid volume surrounding each grid node and V_p is the volume of a single particle.^[10]

In the four-way coupling context, the inter-particle stress force \mathbf{F}_{coll} should be added to the momentum equation (14) as a source term,^[11] while the momentum equation explicitly should account for the presence of particles through the fluid volume fraction $\alpha_f = (1 - \alpha_p)$. Equations (13) and (14) are thus reformulated in a way similar to Equations (6) and (7), that is:

$$\partial_t(\alpha_f \rho) + \nabla \cdot (\alpha_f \rho \mathbf{u}) = 0 \quad (17)$$

$$\partial_t(\alpha_f \rho \mathbf{u}) + \nabla \cdot (\alpha_f \rho \mathbf{u} \mathbf{u}) = -\nabla p + \nabla \cdot \boldsymbol{\tau} + \mathbf{F}_b + \mathbf{F}_{ip} - \mathbf{F}_{coll} \quad (18)$$

The above system of equations becomes pretty much the same as the two-fluid formulation. Following Harris and Crighton,^[12] the fluid-independent force \mathbf{F}_{coll} is made dependent on the gradient of the so-called inter-particle stress, π , using $\mathbf{F}_{coll} = \nabla\pi/\rho_p\alpha_p$. The continuum particle stress model is based on Snider's^[13] proposal:

$$\pi = \frac{P_s \alpha_p^\beta}{\max(\alpha_{cp} - \alpha_p, \varepsilon(1 - \alpha_p))} \quad (19)$$

where the constant P_s has a pressure unit, α_{cp} is the particle volume fraction at close packing, β is a model constant ($2 < \beta < 5$) and ε is a small parameter of the order 10^{-7} .

FLOW ANALYSIS THROUGH POROUS MEDIA (CCS-EOR)

Background

The potential role of carbon abatement technologies in reducing greenhouse gas emissions has gained increased recognition in the EU and in the US. CCS has been widely recognised as potentially useful in this context, because it is the only industrial scale approach capable of deviating large quantities of CO₂ from the source (Carbon Capture) to beneath the Earth's surface (Carbon Sequestration).

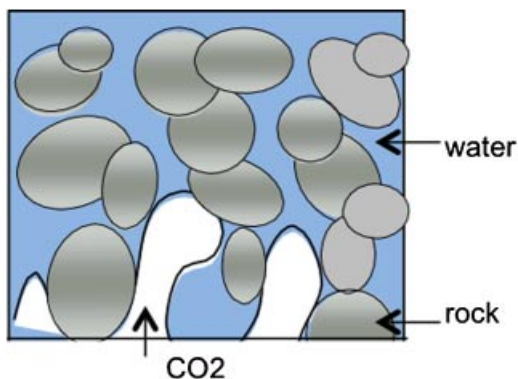


Figure 1. Pore-scale topology.

When considering deep ground storage of CO₂ from coal-based power stations and other sources, the storage sites have to be considerably safe and one has to account for potential leakage over time, either through porous ground layers, or back through the injection shaft. Besides an increase of the energy costs, there are concerns on the long-term fate of geologically stored CO₂. For the development of advanced CCS technologies, a good scientific understanding of CO₂ transport, trapping, dissolution and chemistry under storage conditions is thus a prerequisite. This is clearly within reach of advanced and powerful simulation techniques, provided that the field-scale results are inferred from a correct understanding of the micro-scale mechanisms at play. Model up-scaling should resort to pore-scale Direct Numerical Simulation (DNS) strategies, representing both the multiphase topology and the pore structures (as shown in Figure 1) without relying on homogenised models such as Darcy's law.

Indeed, it is widely recognised that for the scenarios relevant for CO₂ sequestration it is not justified to employ constitutive relations to describe effective relative permeabilities as a function of phase saturation. In reality, relative permeabilities strongly depend on the fine-scale coherence of the spatial phase distribution and on the fraction of trapped fluid, which again depends on the flow history. Consequently one observes hysteresis effects, for example different relative permeabilities and trapped fluid fractions can be observed during imbibition versus drainage as well as for different flow rates. Note that in the context of CO₂ sequestration in particular the quantification of trapped fluid is crucial. However, even if the relevant phenomena can be simulated at the

pore-scale level, the difficult task of upscaling them to a general field-scale description remains. It should be noted that from a physical and numerical viewpoint, the challenges of CCS are very similar to those of EOR and progress made in either field directly benefit the other.

DNS of the Flow Through Porous Media

As mentioned above, DNS alleviates the major drawback of phase averaging since it accounts explicitly for porous medium heterogeneity and enables solving micro-boundary layers at the pore scale. This in turns allows accounting for pore-scale viscous effects, fingering and diffusion, wall shear stress, mass transfer across pore walls, heat transfer at the pore scale, including conjugate heat transfer between pore solids and external fluid (carbon dioxide) exchange and momentum mixing in pores.

The way pore-scale DNS is performed in the CMFD code TransAT is based on two approaches: the Immersed Surfaces Technology (IST) for rock pores with sharp edges, and the granular particle method for sand-type of soils. In IST the solid is described using a level-set function, denoting the signed distance to the wall; is zero at the surface, negative in the fluid and positive in the solid. The idea is borrowed from ITM's used for fluid–fluid systems (cf. Equations 8–12). IST has the major advantage to avoid having to deal with meshing the pore structures (since these are now described by a smooth function, and solve conjugate heat transfer problems directly. The flow through the porous media (obtained via tomographic data) shown in Figure 2 is an illustrative example. The solid defined by its external boundaries using the level set function is immersed into a Cartesian mesh. The fluid equations are solved considering the porous media wall via the level set function.

The second approach can be employed when the soil is characterised by granular-type of structure, for which the IST is not adequate. Here the porous media is represented by an agglomeration of solid particles loading a packed system (Figure 3). The particles are represented in Lagrangian way—although these are not in motion—and phase-averaged in the Eulerian way to be coupled to the fluid phase. Here the particles are subject to an inter-particle stress (Equation 19). This is the first result ever obtained with such an approach. The next step for both techniques is to extend their use to multiphase (water and oil), multi-component (with CO₂) flow systems with relevance to CCS and EOR.

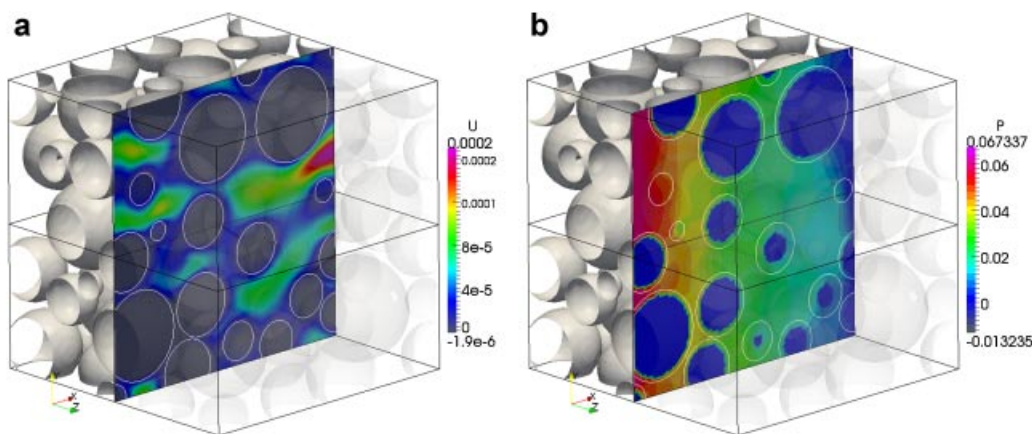


Figure 2. Water flow through a granular porous media (velocity [m/s] and pressure [Pa] contours).

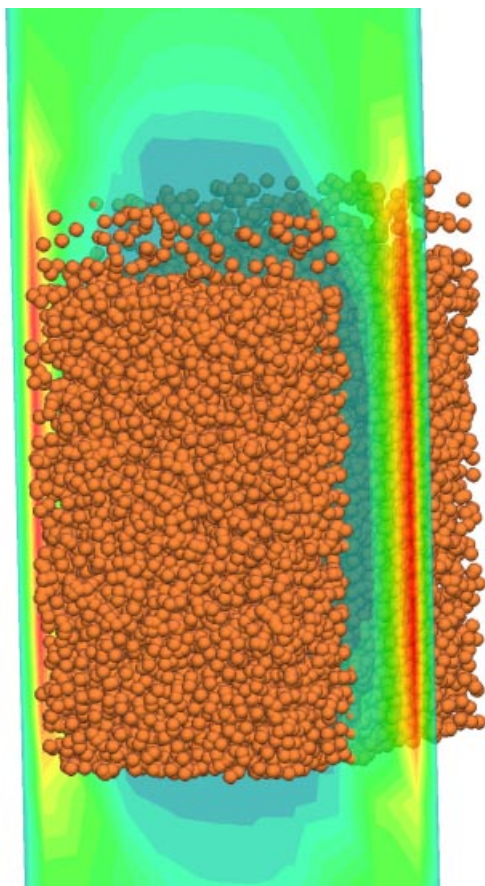


Figure 3. Water flow through a granular porous media (velocity contours): Dense particle flow model.

Multi-Phase Flow Through Porous Media

Porous media flows in the context of CCS or EOR typically involve several liquid or gas phases. For example the recovery of oil can be enhanced by the injection of water, steam or carbon dioxide into the oil reservoir. From a very practical standpoint, to make qualified choices of potential sites for CCS, to estimate their CO₂ storage potential and to quantify the amount of trapped fluid, computational prediction tools are crucial. While the requirements of such simulators are similar to those employed for oil and gas exploration, there exist significant differences. For example, in

CO₂ storage scenarios, residual trapping, dissolution, miscible and immiscible gravity fingering and mineralisation play a leading role. Current models suited for field-scale studies can be ‘tuned’ to some extent, but so far no rigorous upscaling procedure of the above pore-scale phenomena to a continuum-scale description exists. And despite the obvious importance of simulation tools during decision-making processes and reservoir operation, there still exists a great demand for more predictive and general models capable of describing the related complex physical phenomena. This is precisely the motivating point in our research: to improve the understanding of the fine-scale dynamics using efficient and accurate numerical methods that can deal with nonlinear phenomena, such as phase interface propagation and dissolution. Specific challenges include a conservative treatment of evolving menisci, the correct treatment of moving contact lines, dissolution of CO₂ into the brine phase, and gravity fingering. Once such effects can be studied at the pore-scale, consistent upscaling becomes possible allowing for field-scale simulations of practical relevance.

A two-dimensional illustrative example of a gravity fingering instability is shown in Figure 4, where two liquids of different densities flow through an array of cylinders under gravity. The denser liquid in red forms fingers that penetrate into the lighter phase in blue. This limits the effectiveness of the recovery process, as a significant amount of the lighter liquid remains trapped inside the cylinder array. The simulation was performed using IST for the cylinders and the level-set interface tracking method to capture the fingering instability.

Multi-Phase, Multi-Component Flow Through Porous Media

In this section we increase the problem complexity by considering a multiphase, multicomponent flow through a porous media. The context is of direct relevance to CCS or EOR; in the latter CO₂ is injected in the well to boost the oil from the pores. A thin liquid film flows in a porous media in a 2D domain of 20 mm × 10 mm, discretised using 50 × 100 Cartesian cells. Water flows vertically at 0.01 m/s from the upper-left corner of the domain and leaves the domain from the right boundary. All other boundaries are impermeable walls. The gas phase is initialised with volume fractions of 0.99 and 0.01 for CO₂ and CH₄, respectively. The liquid phase is initially composed only of H₂O. The gas-liquid interfacial model does not include phase-change. The gas-phase components, however, can dissolve into the liquid following Henry’s law (where the gas solubility is proportional to its partial pressure). The model using the level set technique to separate the water from the gas

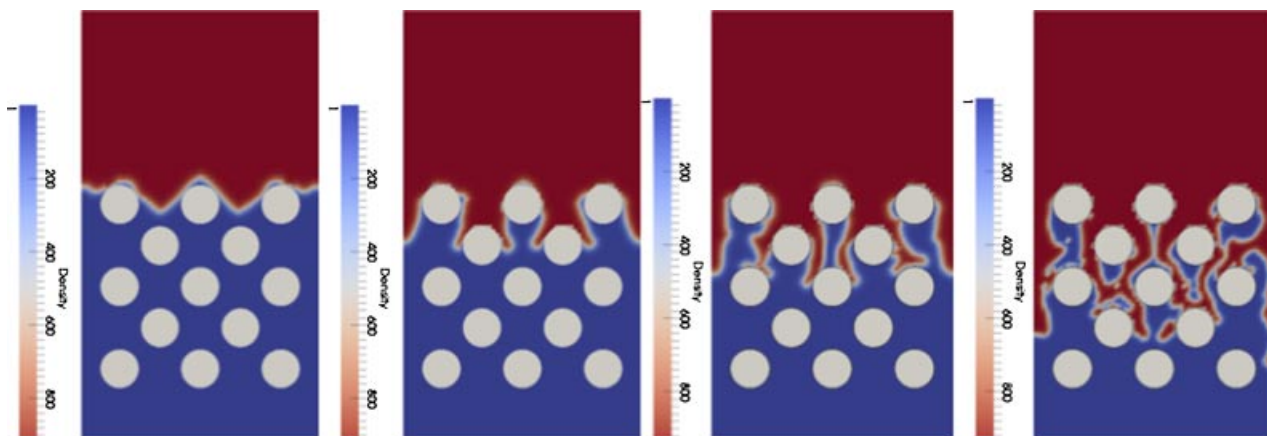


Figure 4. Two-phase flow through an array of cylindrical porous media. Interface Tracking Method.

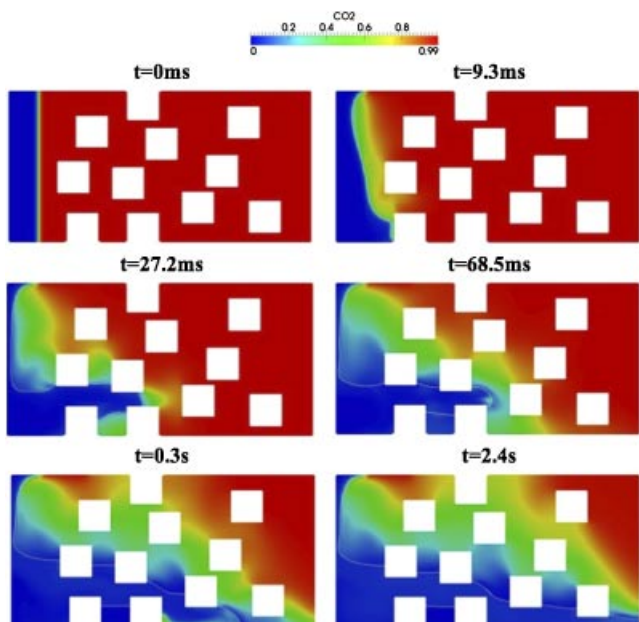


Figure 5. Multiphase multicomponent flow across a porous medium.

phases; the latter are treated separately by solving a transport equation for each of the species. The porous media is represented by an ad hoc structure constituted by random cubical obstacles; it could have been similar to the array of cylinders presented previous to this section.

Initially the water front moves with gravity effects downward before penetrating the structure (Figure 5); it is perhaps important to note that in the level set approach used here, a triple-line model is included to account for wetting of the front on the rock pores. The model is based on the triple force decomposition of Young's; see Friess and Lakehal^[14] for more details. It is remarkable to note that the chemical reaction between the two gaseous species operates from the water front inward to the gas mixture phase. Note that there is no mass diffusion allowed between the gaseous phases and the liquid. CO₂ phase is consumed slowly as the water front evolves within the structure. While this example is an idealised configuration, the results suggest that this type of simulations could now be employed to predict real CCS problems.

DESTRATIFICATION IN LNG TANKS

Storage tanks for Liquefied Natural Gas (LNG) are usually filled with LNG of different densities. Stratification may occasionally lead to rollover and rapid tank pressure rise, which could be harmful to the filling operation and may break the flow assurance. The LNG stations should be properly designed to prevent the venting of natural gas from LNG tanks, which can cause evaporative gas emissions and result in fluctuations of fuel flow and changes of its composition. LNG tanks commonly have two types of filling nozzles, top and bottom. Choice of filling point depends on whether the cargo LNG is more or less dense than the LNG already in the tank (the heel). Basically, bottom filling of lighter LNG and top filling of heavier LNG are recommended. Stratification depends on the nozzle, the initial density difference, the depth of the heel and the filling rate. Also, the injection of a lighter LNG at the bottom of a stratified storage tank leads to large-scale motion inside the tank, which affects the rate of mixing and time for stratification.

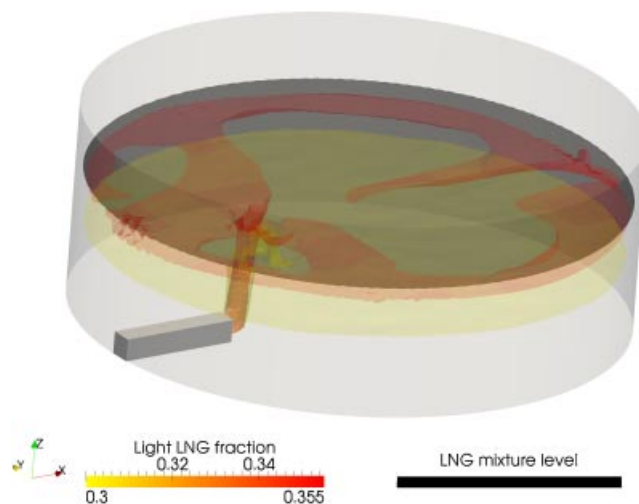


Figure 6. Volume fraction contour of lighter LNG during reception into storage tank.

The problem was borrowed from the work of Koyama^[15] who used the two-fluid, six-equation model. Instead in TransAT we have tested for the same problem using two alternative strategies explained above: the N-phase mixture model in which the inter-phase slip is algebraically prescribed, and the level set technique providing a clear distinction of the front. Turbulence was in all cases modelled using a simple URANS approach modified to cope with buoyancy effects. Right at the injection and depending on the initial temperature difference and injection rate, large scale structures are observed with size up to half of the tank. These energetic events tend to mix very strongly the phases, causing delays in the final desired stratification of the tank. These large-scale motions could be seen from the velocity field depicted in Figure 6. This effectively mixes the LNGs of different densities and de-stratifies the storage tank. The time evolution of the LNG density profile is shown in Figure 7. The CFD results agree with experimental data taken from Koyama.^[15] When use was made of the N-phase model, the results were not as good.

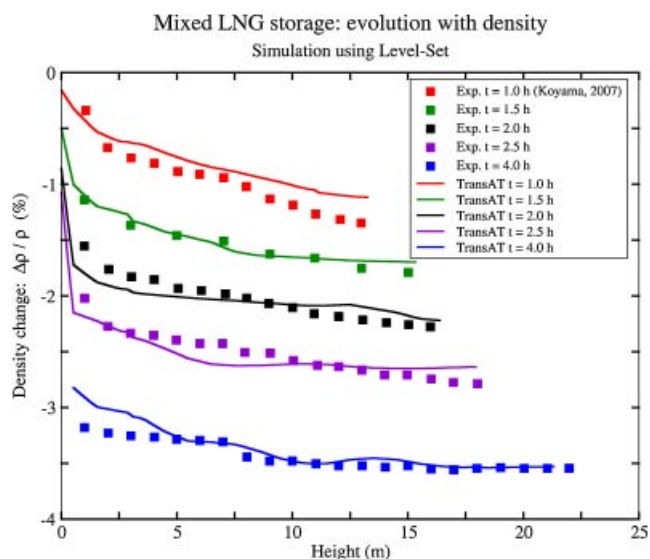


Figure 7. Mixed LNG storage—Comparison between calculated and measured density profile.

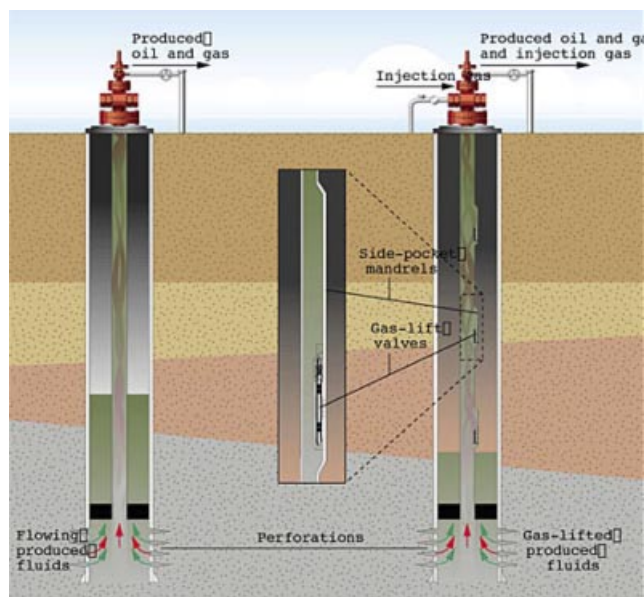


Figure 8. Cross-section of wells employing gas lift. Courtesy: Schlumberger.

GAS LIFT

In the gas-lift technique, gas is injected at the bottom of a production pipe (through which oil and water are flowing) in order to reduce the gravitational pressure drop in the well. This results in an increase of the oil flow rate in the pipe. In practice, gas is injected from valves attached to the pipe wall, which generates large bubbles. Previous work^[16] with water and air indicates that the gas-lift efficiency can be improved by injecting small bubbles. The gravitational pressure drop is then reduced because: (i) the rise velocity of small bubbles is lower, and hence the residence time and void fraction in the pipe are higher, (ii) small bubbles are more evenly distributed over the cross-section of the pipe, which increases the gas void fraction and (iii) small bubbles postpone the transition from bubbly flow to slug flow, which is an undesirable operating condition for gas-lift. A schematic of the gas-lift technique is shown in Figure 8.

We have conducted a preliminary feasibility study, using the level-set technique to track the gas bubbles injected at the bottom of a vertical riser filed with water; no oil is considered. The simulation was performed under 2D axisymmetric conditions. The gas is injected at the bottom (see Figure 9) at different flow rates, and the pressure drop is calculated for different values of the gas superficial velocity at the injection nozzle. The form of the nozzle is also idealised, although we have ensured that the gas flow is injected downward. The results shown in Figure 9 for variable gas flow rates indicate how the model is capable of predicting bubbles of different sizes rising in the pipe at different speeds and taking specific zigzag paths. Interestingly, with the level set method there is no need to adjust the drag or lift coefficient, the latter is known to heavily affect the motion of the bubbles, drifting them towards the wall or towards the core flow, depending on the size. These results should of course remain qualitative only. More importantly from a global viewpoint, the CFD prediction is in line with the experimental results, in that injecting even a relatively small quantity of gas tends to significantly reduce the pressure drop in the riser, as shown in Figure 10.

MULTIPHASE FLOW IN VERTICAL PIPES

Motivations

As stated in Introduction Section, gas-liquid flow in pipes is of great practical importance in petroleum engineering, in particular for separation and transportation. Mixtures of gas and liquids (light and heavy components of oil, solid particles, hydrates, wax, condensate and/or water) are produced and transported together under various topologies (e.g. bubbly, slug, annular, mist) (Figure 11). In addition, the relative volumetric fraction of the phases can change along the pipes either because of heat addition, heat exchange between the phases or flashing due to depressurisation. In vertical pipe flows, for example risers, the flow regime identification (up to three main phases, plus when possible sand and hydrates) is critical for the success of drilling and production. The main task in modelling multiphase pipeline flows is the identification of the flow-regime map.

Current predictive tools for multiphase flow and heat transfer in pipes are based on the two-fluid, six-equation model, in which

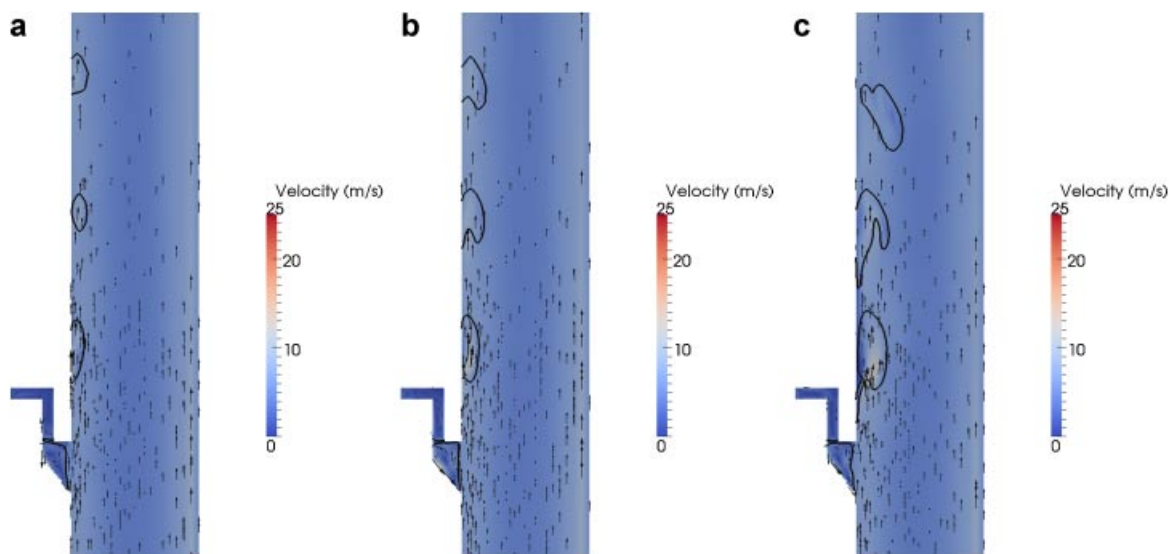


Figure 9. Gas injection in a vertical pipe for superficial velocities of 0.2, 0.5 and 1 m/s at the injection nozzle. Black contours show the gas bubbles.

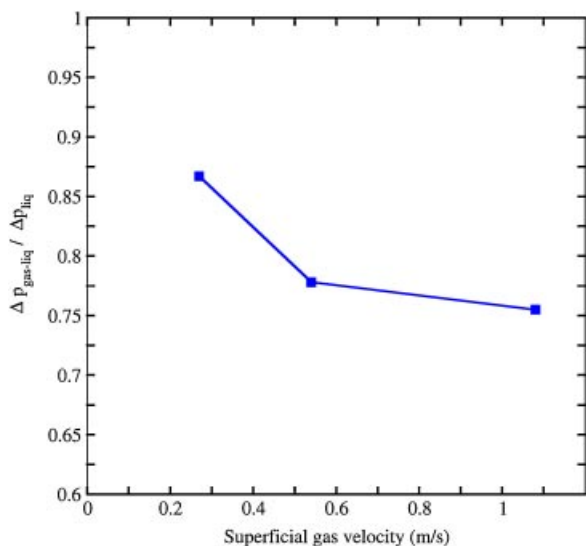


Figure 10. Pressure drop for increasing superficial gas velocity at the injection nozzle.

the conservation equations are solved for each phase. In the oil and gas industry this model is reduced to 1D, and is commonly referred to as the ‘Mechanistic Model’. Solution of the Mechanistic Model equations requires specification of closure relations for flow characteristics such as local velocities, wall shear stress, liquid holdups, etc. These closure relations carry the largest uncertainties in the model and are typically empirical, making use of over-simplified assumptions; in particular, the geometry of the vapour/liquid interface is always idealised, for example spherical or bullet-shaped bubbles, smooth or sinusoidal wavy liquid films, spherical or elliptic droplets. The physical reality of the situation is

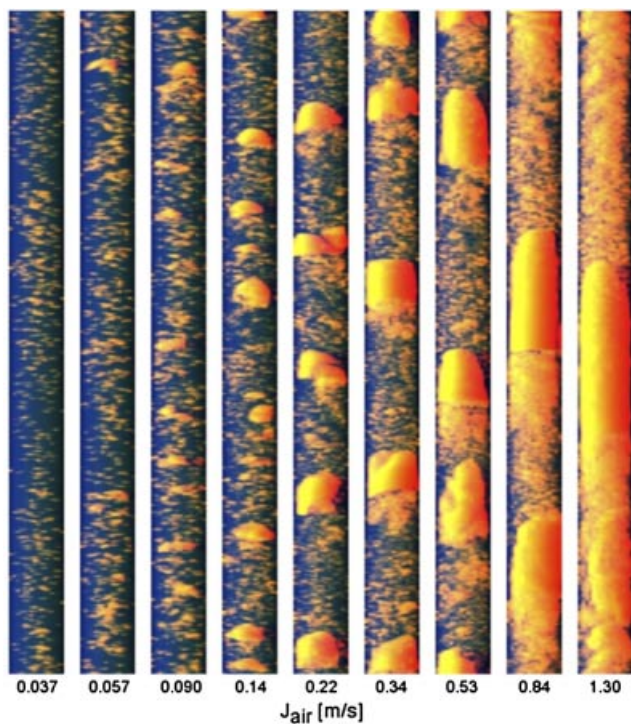


Figure 11. Flow regime variation in a vertical pipe with gas superficial velocity (with permission^[34]).

much more complex, as shown in Figure 11, displaying the various flow regimes encountered in ‘controlled’ laboratory experiments. Furthermore, the closure relationships are often developed from low pressure, small diameter pipe (typically 25–75 mm) data using synthetic oil and air, which does not simulate actual field conditions, making upscaling to predictive codes highly uncertain. All these uncertainties in the closure relations reflect on the overall accuracy of the predicted figure of merit, for example pressure drop. For example, the codes adopting the Mechanistic Model and used by the oil industry could predict the pressure drop in a vertical riser with an error of more than 60.%^[6] The closure relations are flow regime dependent and it is well known that flow regimes in large pipes (300 mm diameter, like deep-sea riser pipes) differ significantly from those in smaller pipes. For example, slug flow is replaced by cap flow in large pipes because of large-bubbles instabilities. The complexity increases when more than two phases evolve in the pipe, for example gas, water and oil. In this case the flow regime map is expected to feature a broader domain for churn and annular flow, the topology of which remains difficult and expensive to investigate experimentally.

In horizontal pipe flows, the main open issue requiring better understanding is the transition from stratified flow to slug flow.^[17] Slug flow is a commonly observed pattern in horizontal and low upslope gas liquid flows. The regime is associated with large coherent disturbances, due to intermittent appearance of aerated liquid parcels filling the pipe cross-section. As these aerated liquid parcels travel downstream the pipe, large pressure fluctuations and variations in flow rates could occur, which could affect process and separation equipment. Our recent CMFD results^[18] of flow transition in horizontal pipes has clearly shown the importance of relying on advanced 3D simulation techniques, and has shed light on subtle mechanisms in association with surface deformation, sealing and slug displacement.

Air–Water Flow in a Vertical Pipe

Measurements of a mixture of gas–water flowing in a vertical pipe of 6.7 cm diameter and 6 m length with various superficial air and water velocities were conducted at the Chemical Engineering Laboratory of the University of Nottingham, UK.^[19] Liquid and air were mixed at the bottom of the pipe by a special mixing device. The liquid enters the mixing chamber from one side and flows around a perforated cylinder; air is injected through a large number of 3 mm diameter orifices, thus, gas and liquid could be well mixed at the test section entry. Inlet volumetric flow rates of liquid and air were determined by a set of rota-meters. Gas void fractions were measured at a height of 5 m using a wire-mesh sensor.

The bubbly flow cases (1st two panels of Figure 11) were simulated and published in another contribution,^[18] and are thus not discussed here. Two cases were reproduced numerically using the code TransAT: In Case 1, the gas superficial velocity is $J_G = 0.57$ m/s, for a comparable liquid superficial velocity: $J_L = 0.25$ m/s. According to Szalinski et al., this is a flow featuring a clear Taylor bubble, corresponding to the 7th panel of Figure 11. Case 1 is an intermittent slug flow with by a cloud of smaller bubbles trapped in the wake of the large cell. In Case 2, the gas and liquid superficial velocities are $J_G = 45$ m/s and $J_L = 10$ m/s, respectively, which corresponds to the annular flow regime, as in the rightmost panel of the figure.

3D Slug Flow Simulation Results

Case 1 includes the formation of air slugs or Taylor bubbles travelling upward along the pipe, which makes it more complicated

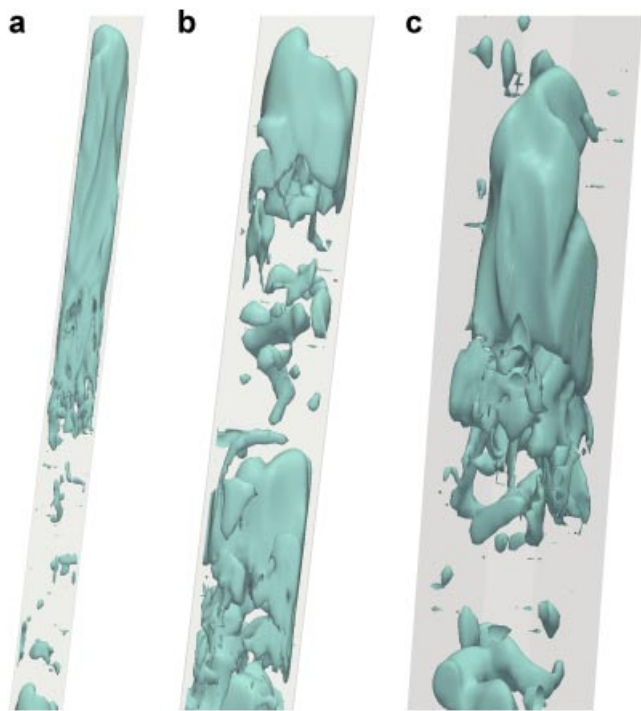


Figure 12. 3D LEIS simulation (Level Set + LES) of a transition to slug flow.

to model because of the simultaneous presence of large and small bubble structures trapped in the wake, and associated unsteady ‘meandering’ of the flow and more active turbulence generated due to the interaction of the phases, and between the aerated structures of different size. The chosen pipe length is only 3.1 m to ensure sufficient grid resolution and reasonable CPU time. The Algebraic slip model has been used although it is well known that this approach applies only for flows laden with small bubbles of sizes comparable to the grid size. The modelling of the drift velocity is another issue, since it requires the average bubble radius. Although we are aware that this class of models cannot be applied for slug flows, we have used it nonetheless, assuming a bubble radius of 3.0 mm (otherwise the model crashes).

The 3D simulation was performed on a HPC supercomputer with 128 Processors. Level set has been combined with full LES for turbulence (the combination is known as LEIS^[3]), using the WALE subgrid-scale model.^[20] The grid consists in 3 million cells. The Immersed Surface Technique (IST) was employed, in that a CAD representing the pipe has been simply immersed in a Cartesian grid. Near-interface treatment of turbulence follows the model proposed by Liovic and Lakehal^[21] and Reboux et al.^[22] High-order schemes were employed, up to 3rd-order RK for time marching, and 2nd-order central scheme for convection fluxes; the Quick scheme was used for solving the level set equation. The time-step varies in time (bounded by convection, diffusion and surface tension CFL-like limiters ~ 0.4 – 0.7) depending on the topology of the flow, decreasing when small bubbles appear, down to 10^{-5} s sometimes. Understandably this first attempt has been made possible thanks to the available HPC resources only. The simulation of 6 s reproducing four slugs required 22 H on the HPC supercomputer.

Figure 12 clearly shows that the LEIS approach provides a rich picture of the flow as might be in reality and is qualitatively much closer to the experiment: cf. 4th panel of Figure 11. Slugs of different sizes and elongations form naturally without triggering

their onset, occupying the entire pipe and travel upwards. Swarms of bubbles are also generated in the wake, populating the area between the Taylor bubbles. Our videos show actually that the bubble wake is primarily a result of fragmentation of the Taylor bubble wake due to strong interfacial shear dominating surface tension. Despite the qualitative picture, this grid is not sufficient to resolve the cloud of bubbles as depicted in the experimental images. Furthermore, because of the grid resolution, grid-size bubbles formed tend to disappear. Also, time averaged profiles could not be generated, because steady-state ergodic conditions require averaging over at least 10 Taylor bubbles travelling along the pipe.

3D Annular Flow Simulation Results

For the annular flow regime (Case 2), the dimensions of the pipe were reduced to 3 cm \times 100 cm. With a grid of 800 000 points, the simulation required 32 h to perform 20 000 iterations on a HPC cluster, using 128 cores. The numerical method and parameters were the same as for the slug flow simulation discussed above. The resulting time step was approximately 6×10^{-6} s. Here, too, the level set approach was used in connection with LES for turbulence; basically the same model setup as in the previous slug flow. In reality the film thickness is quite small compared to the value set in this case, otherwise a much larger grid would be required to resolve the film.

Density contours marking the interface and cross-flow velocities vectors of the air–water pipe flow are shown in Figure 13. The coherent structures of the water film can be seen in both streamwise and spanwise directions. Only in a few locations we could observe water parcels migrating to the core flow. This is a remarkable result that has been so far with the realm of speculation only. The evolution of the water film thickness on the walls is reported in Figure 13 at different cross-sections, indicating that the flow is not yet fully developed and the comparison with the data of velocity and density profiles would require a longer pipe. Although presented as a *proof-of-concept* only, these LEIS results are very encouraging and demonstrate TransAT’s capabilities for simulating multiphase vertical pipe flows. Such an approach provides a novel versatile method for exploring/explaining riser flows.

Figure 14 shows three cross-flow locations of the pipe, featuring the liquid film deformation. It is interesting to note that there is a certain radial coherence of the events. Occasionally we could observe detached droplets migrating to the core flow.

Figure 15 depicts the evolution of the liquid film thickness in the annular flow regime taken at $z = 70, 80$ and 90 cm. The plotted values are normalised by the initial liquid film height. One observes how intense the deformation of the interface could be, with fluctuations around the mean reaching $\sim 400\%$. The frequency of the coherent waves could be extracted from the results below, indicating that it may change with time by up to one order, that is $125 < f < 275$ Hz.

SUBSEA HYDRATE FORMATION AND PLUGGING

Background

Subsea hydrate formation may cause blockages in oil production lines, and as such it remains today one of the main concerns to deepwater field developments. The present strategy of operators is commonly focused on the deployment of prevention methods that aim at producing outside the hydrate domain. This can mainly be achieved via pipeline insulation (for oil systems) or chemical injection (for gas systems). Another strategy is to produce inside the hydrate domain and transport the hydrate phase as slurry of

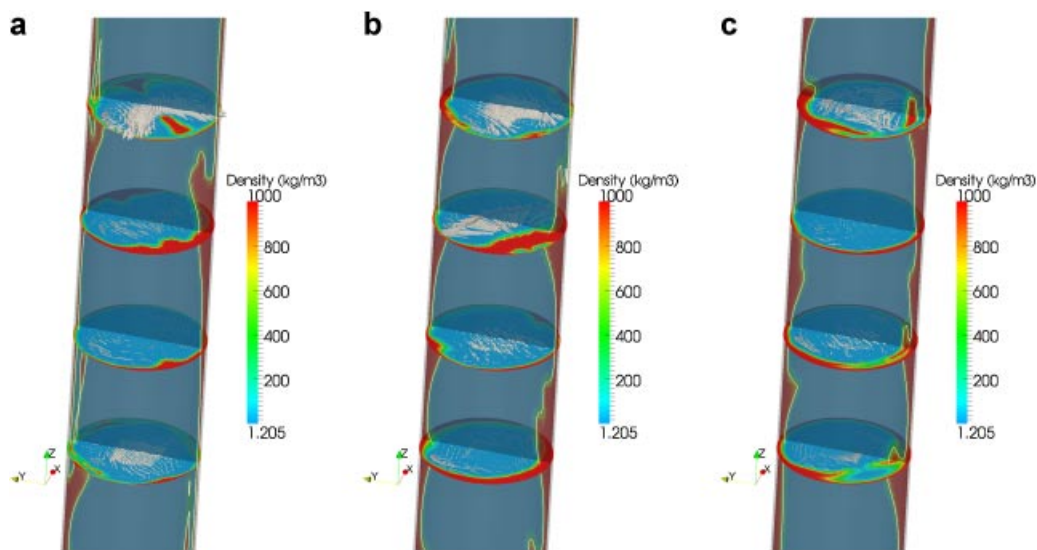


Figure 13. 3D LEIS in the annular flow regime. Snapshots of the flow shown at three different times.

hydrate particles dispersed in the oil phase, which led to developments of Anti-Agglomerant. Even so, injection of such chemicals remains marginal. Similarly, natural surfactants (e.g. asphaltenes, resins, etc.) present in most of black oils were also considered as potential agents enabling hydrates to be transported as slurry. Operators envisage taking advantage of such surfactant properties to ensure restarting after a long shutdown.^[23]

Various studies report on crude oils and hydrate control.^[24,25] Most of these studies show results on plugging or non-plugging occurrence in laboratory facilities though under flow conditions inside the hydrate domain.^[26,27] In terms of simulation, 1D models for hydrate-plug formation in flowlines are available, and have been successfully applied for subsea tiebacks. Three-dimensional full CFD predictions are however rare in this area.

Improving the understanding of the flows occurring in risers and associated subsea oil production equipment is becoming important to respond to possible incidents such as the Macondo event. The objective of resorting to detailed CFD is to improve the realism and accuracy of predictions of the behaviour of multiphase flows in risers and to improve the understanding of complex flow phenomena associated with deepsea hydrocarbon spills, including multiphase flow jet evolution, hydrate formation and dissolution, thermodynamics of hydrocarbon mixtures during fast pressure and temperature changes, and transient interaction of plume constituents with the surrounding turbulence. The CMFD

code TransAT is one of the rare tools capable of predicting subsea multiphase hydrocarbon flows. The model is specifically dedicated to N-phase flow systems featuring complex fluid physics, including hydrate kinetics, formation and dissolution, deep-sea thermodynamics, and very complex rheology. In addition, the code is capable of predicting wall adhesion of the hydrates plugging on piping internals.

Hydrate Plugging of Subsea Equipment

One of the key issues in modelling hydrate plugging of flowlines and equipments is to determine whether the hydrates stick (adhere) to the solid wall or not. In the former case, it is also unclear which of the hydrates really do stick: the ones formed by methane phase change in contact with cold water, or those formed by the light components of oil? For the purpose, several models have been developed and implemented in the code TransAT, one of which is based on the stability principle of the hydrates in contact with the walls, combined with an advanced rheology model similar to Bingham's model.^[24] Prior to using the model for hydrate plugging of subsea caps, for example that employed by BP to cap the Macondo blow up, it was first employed to predict the plugging of a vertical riser flow initially filled with oil and water and methane. The pipe dimensions and fluids flow rates are not important: it suffices to show that for the particular thermodynamics conditions selected, one can clearly see the

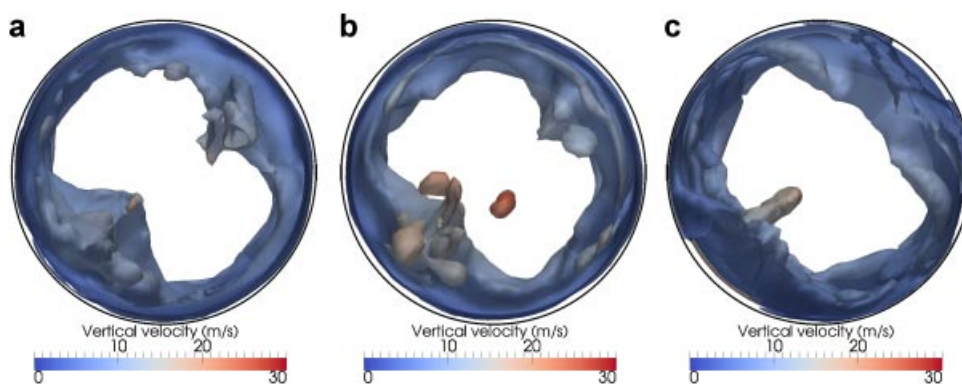


Figure 14. 3D LEIS in the annular flow regime. Snapshots of the pipe at three cross-flow locations.

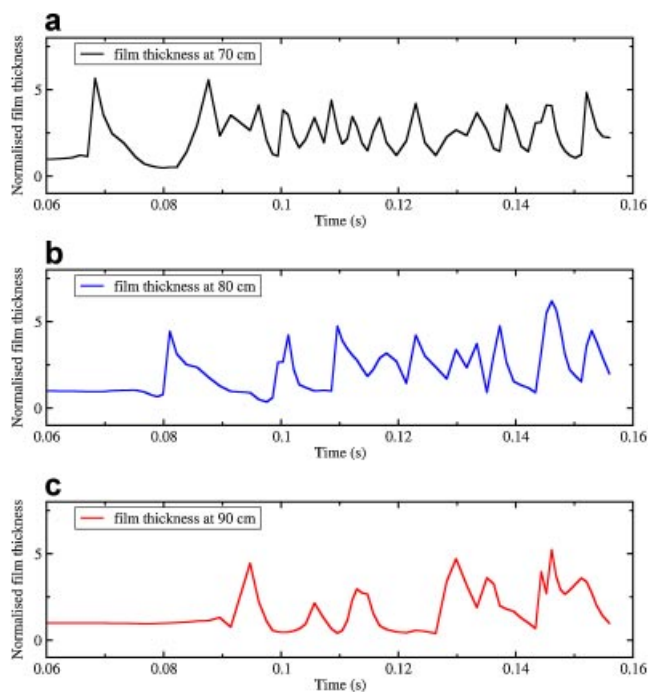


Figure 15. Evolution of film thickness in annular flow regime at $z = 70$, 80 and 90 cm.

nucleation of hydrates in the centre of the pipe developing up to a full plugging (Figure 16, left), as confirmed by the pressure contours at corresponding times (Figure 16, right).

The hydrate model implemented within the N-phase mixture model was then used to predict the plugging in the canopy employed by BP to collect the oil in the aftermath of the Macondo event, for which experimental data of the canopy are available online (Figure 17, left). TransAT has been used to predict hydrate-induced plugging in the canopy taking hypothetical values only, without any specification or information from any source. 2D simulations were conducted first, using the N-phase model described earlier to deal with the various flow components. The model was used in combination with URANS for turbulence. The right panel of Figure 17 shows a snapshot of the flow featuring only oil (coloured) and water (blue), before activating the complete hydrate formation/adhesion/melting module. The

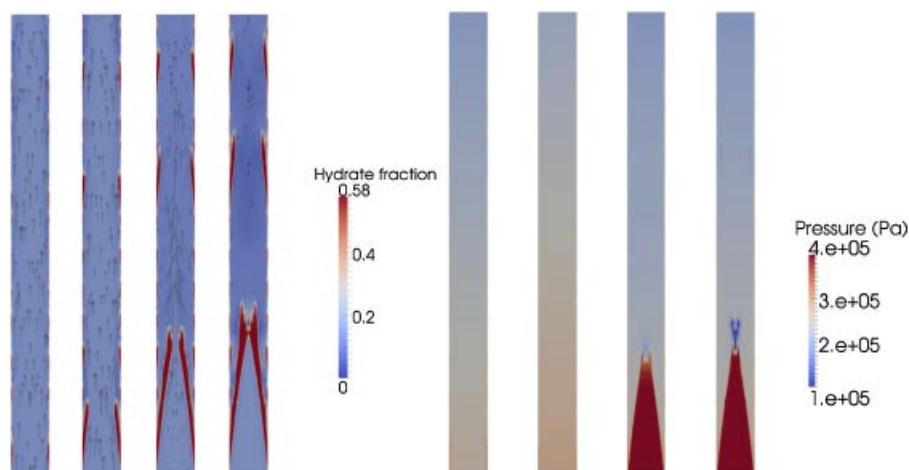


Figure 16. Hydrate formation and corresponding pressure in the pipe, at different times.

result (right panel) shows that the flow escapes partially from the canopy. These first results have indicated that the jet flow features strong unsteadiness and could only be well predicted using a time dependent approach; steady-state simulations are simply meaningless in this context. Since use of LES is prohibitive for similar problems, we have extended the model to couple the N-phase with hydrate module with V-LES, or Very Large Eddy Simulation, a strategy bridging LES with URANS that can be competitively advantageous for very high Reynolds number flows.^[18,28]

In a second step, use was made of the complete model now under V-LES to better capture flow unsteadiness. The results in Figure 18 suggest that the stability model employed in connection with Palermo's rheology model renders well the adherence of the hydrates on the canopy internals, leading to a blockage of the flowlines that evacuate the oil via the riser (left column). The figures show the sequence beyond blockage, when oil starts escaping from the canopy. To try and prevent blockage, it was proposed to inject methanol from various small nozzles inside the canopy (not shown)—the effect of methanol is to locally lower the critical temperature of hydrate formation. In the presented case, although some hydrates still adhere to the walls, the riser does not get blocked and almost no oil escapes the canopy (Figure 18, second row). Clearly, detailed CMFD provides an invaluable prediction tool for this problem. For more realistic flow conditions at the riser's exit, however, this 3D simulation should be coupled with a 1D code to simulate the entire process: from oil collection near the source to its transport to the surface.

PARTICULATE FLOWS

Background

Particle-laden flows are of great practical importance in oil and gas engineering. The formation and accumulation of black powder in pipelines, for example, may be very harmful for hydrocarbon transportation installations and engineering studies are heavily investing in computer-based predictive strategies to anticipate hypothetical black-powder slug formation and develop fast and efficient removal techniques to operate in time.^[29,30] Similarly, promising oil extraction techniques such as hydraulic fracturing involve transporting a proppant, such as sand, into rock fractures to keep them open and facilitate oil flow.^[31] Because of the strong interactions between the fluid carrier phase and the solid particles, advanced numerical methods are often needed for this class of

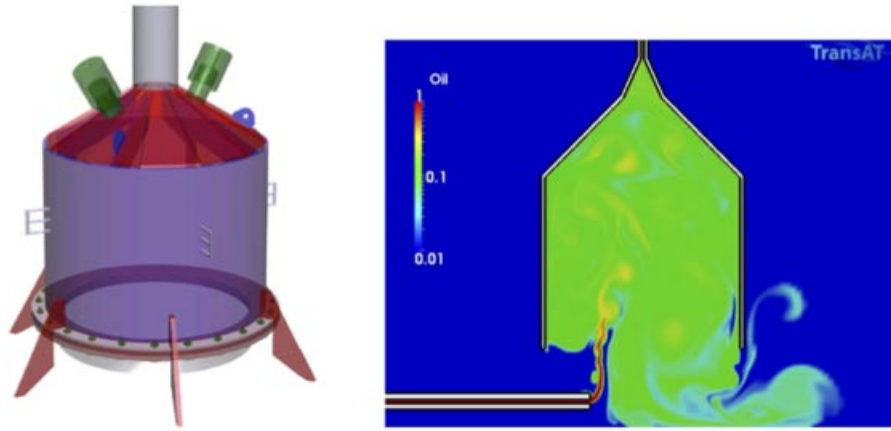


Figure 17. BP canopy used to resume oil spill in Macondo well. Flow simulated with TransAT (oil and water only). Only a portion of the riser is considered.

flows: Lagrangian particle tracking including four-way coupling instead of average Euler–Euler formulations, Large-Eddy Simulation (LES) instead of RANS, and transient rather than steady-state simulations.

Single-Phase Dense Particle-Laden Flows

To validate TransAT’s fluid/particle interaction models, simulations were performed for one experimental condition (Narayanan and Janssen, 2009) of gas flow through a 6-inch horizontal pipe

at a system pressure of 10 bars and gas temperature of 20°C. An initial mass of 200 g of particles (with sizes in the range 200–400 μm) lies at the bottom of the pipe. The four-way coupling model (Equations 17 and 19) for dense-particle simulations was used. Turbulence was resolved using the V-LES method. Consistently with what was observed experimentally, the particles are dragged along by the flow but remain near the bottom of the pipe. The critical velocity (defined here as the gas velocity needed to transport 10% of the initially injected dust mass over the 6.1 m

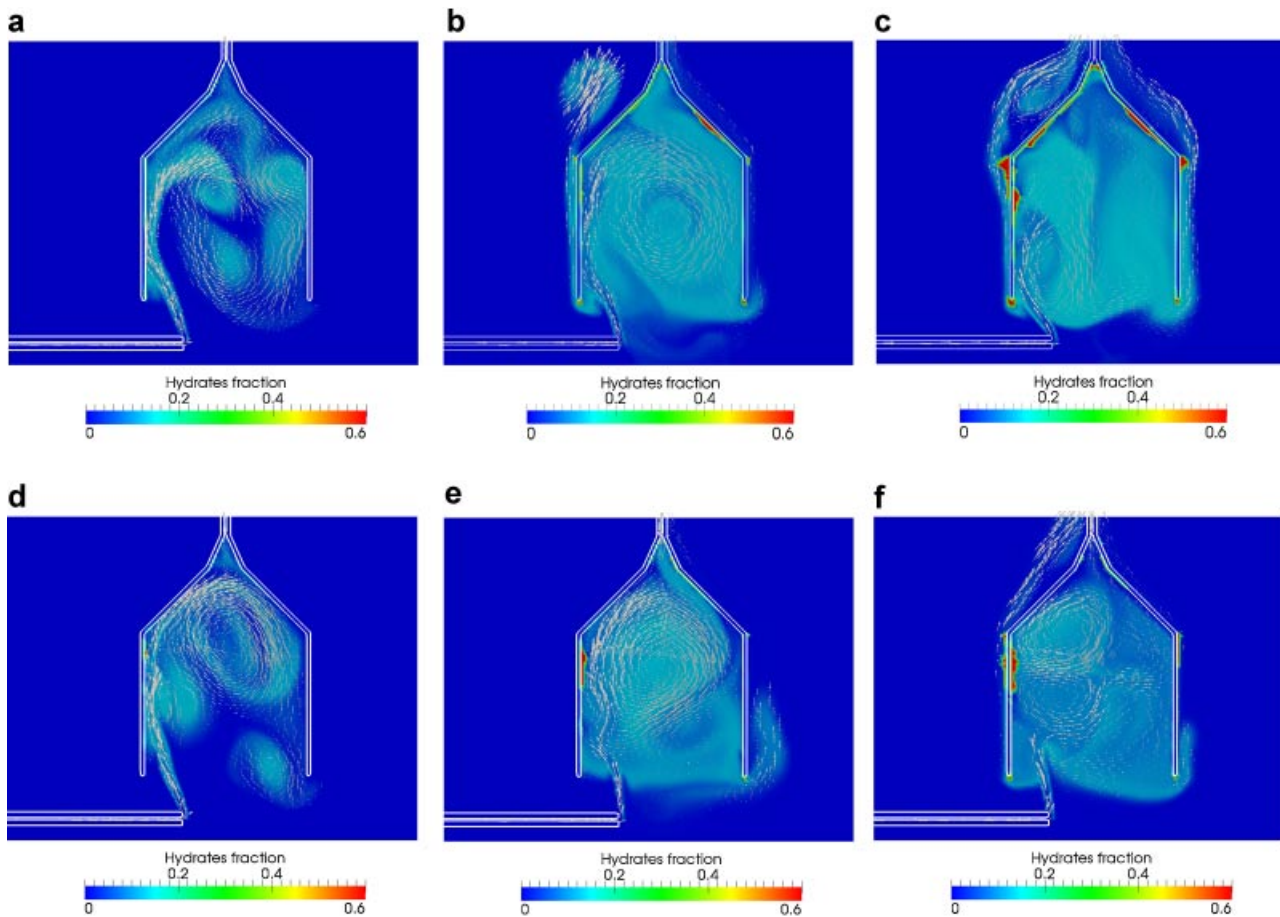


Figure 18. BP canopy used to resume oil spill in Macondo well (oil, water, methane and hydrates). First row: without methanol. Second row: with methanol.

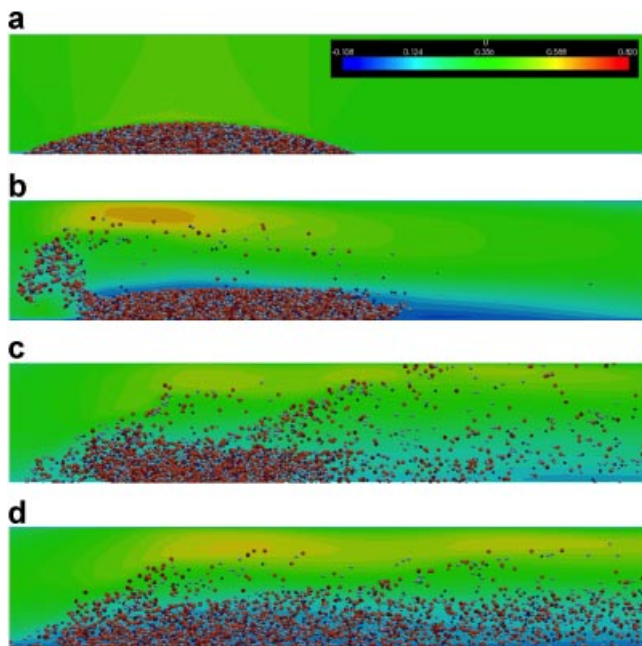


Figure 19. Black powder re-entrainment in pipe flow. Snapshots are shown at different times. Particles are coloured by size.

length of the pipe) was found to be within 10% of the 3 m/s found experimentally.^[32] Under different conditions, with larger particles, the turbulence within the carrier phase simulated by V-LES generated sufficient flow unsteadiness to lift up the particles and move the deposited bed through re-entrainment in the core of the flow. Snapshots of the flow are shown in Figure 19, depicting particle concentration in the bed (coloured by their size) and the flow developed through the interaction with the carrier phase.

The distribution of particles in the vertical direction was validated against experimental results from Laín and Sommerfeld.^[33] The setup is a 2D channel of height 3.5 cm and length 6 m. The particles have a diameter of 130 μm and a density of 2450 kg/m^3 . The void fraction of the inflow fluid is set to 0.00093, with a mean inflow velocity of 20 m/s in the x -direction and a standard deviation of 1.6 m/s in x and y directions. The initial angular velocity of the particles is set to 1000 s^{-1} . A grid size of 125×34 was used. The simulations were run using the two-way coupling model and a Langevin forcing to account for the effects of turbulence on the particles. The wall collision model for particles from Laín and Sommerfeld^[33] was used to take wall roughness into account. The results in Figure 20 show excellent agreement between the fluid and particle velocity profiles measured experimentally and that simulated by TransAT. The simulation also accurately predicts the pressure drop along the channel (the results are shown for a wall roughness gradient of 1.5).

CONCLUSIONS

The progress made in predicting multi-phase flows with high fidelity in the context of oil and gas problems has been reported. Complex multi-phase, oil and gas problems are shown to be within reach of modern 2D and 3D CMFD techniques implemented in the code TransAT. The examples were presented to demonstrate the capabilities of CMFD simulations in general and TransAT in particular. Deeper insight into each individual problem would of course require a dedicated study to exploit the rich database

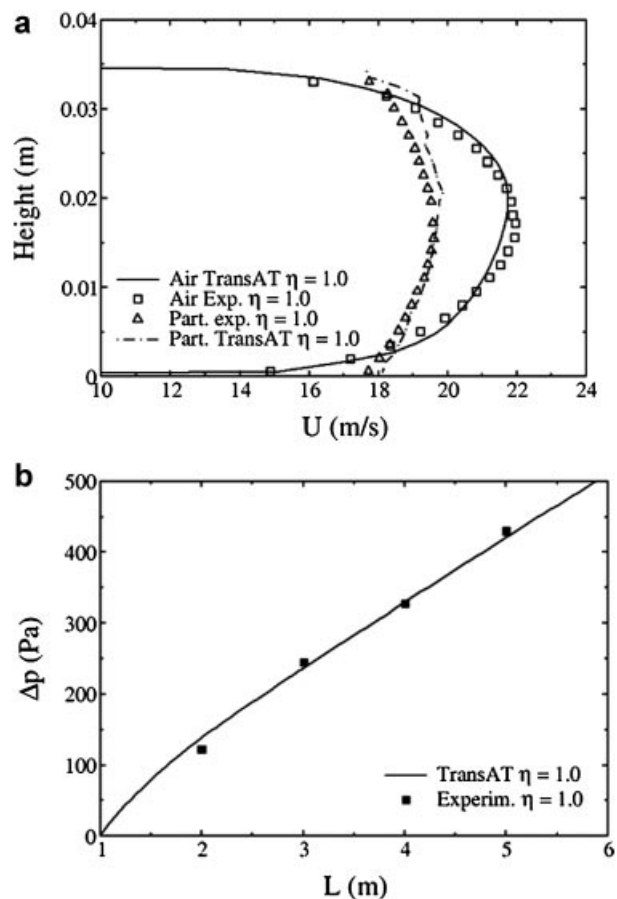


Figure 20. Mean air and particle velocity profiles (left). Mean pressure drop at streamwise locations L (right).

generated in the simulations. Most of the models can be further refined and adapted for various scenarios. It is true that various limitations and roadblocks need to be alleviated before such CMFD techniques could be efficiently used and provide a real added value to the various processes, as is the case today with 1D codes like OLGAs, LEDAFLOW, etc. Present effort is dedicated to the coupling of TransAT with 1D codes to cope with specific problems requiring more than one single strategy.

REFERENCES

- [1] G. F. Hewitt, *Nucl. Eng. Des.* 2005, 235, 1303.
- [2] S. Nestic, *Corros. Sci.* 2007, 49, 4308.
- [3] D. Lakehal, *Nucl. Eng. Des.* 2010, 240, 2096.
- [4] A. Ansari, N. Sylvester, C. Sarica, O. Shoham, J. A. Brill, *SPE J.* 1994, 152, 143.
- [5] J. Xiao, O. Shoham, J.A. Brill, *Proc. SPE ATCE*, New Orleans, LA, 23–26 September 1990.
- [6] R. Belt, B. Djoric, S. Kalali, E. Duret and D. Larrey, *Proc. Multiphas. Flow BHR*, Cannes 2011.
- [7] M. Manninen, V. Taivassalo, *VTT Pubs.* 1996, 288, 67.
- [8] D. Lakehal, M. Meier, M. Fulgosi, *Int. J. Heat Fluid Flow* 2002, 23, 242.
- [9] M. Sussman, P. Smereka, S. Osher, *J. Comput. Phys* 1994, 114, 146.
- [10] C. Narayanan, D. Lakehal, *Phys. Fluids* 2006, 18, 093302.

- [11] D. Gidaspow, *Appl. Mech. Rev.* 1986, 39, 1.
- [12] S. E. Harris, D. G. Crighton, *J. Fluid Mech.* 1994, 266, 243
- [13] D. M. Snider, *J. Comput. Phys.* 2001, 170, 523.
- [14] H. Friess, D. Lakehal, 3rd ICHMT symposium on advances in computational heat transfer, vol 2, 2004.
- [15] K. Koyama, *Syst. Modell. Simul.* 2007, 2, 39.
- [16] S. Guet, G. Ooms, R. V. A. Oliemans, R. F. Mudde, *AIChE J.* 2003, 49, 2242.
- [17] P. Valluri, P. D. M. Spelt, C. J. Lawrence and G. F. Hewitt, *Int. J. Multiphas. Flow* 2008, 34, 206.
- [18] D. Lakehal, M. Labois, C. Narayanan, *Prog. Comput. Fluid D.* 2012, 12, 153.
- [19] L. Szalinski, L. A. Abdulkareem, M. J. Da Silva, S. Thiele, D. Lucas, V. Hernandez Perez, U. Hampel, B. J. Azzopardi, *Chem. Eng. Sci.* 2010, 65, 3836.
- [20] F. Nicoud, F. Ducros, *Turbul. Combust.* 1999, 62, 183.
- [21] P. Liovic, D. Lakehal, *J. Comput. Phys.* 2007, 222, 504.
- [22] S. Reboux, P. Sagaut D. Lakehal, *Phys. Fluids* 2006, 18, 105105.
- [23] N. F. Nygaard, *4th Int. Conf. on Multiphase Flow*, Nice, June 1989.
- [24] T. Palermo, R. Camargo, P. Maurel, J. L. Peytavy, *11th Int. Conf. on Multiphase Flow*, San Remo, 219, 2003.
- [25] R. Camargo, T. Palermo, *Proc. of the 4th Int. Conf. on Gas Hydrates*, Yokohama Symposia, Yokohama, Japan, 19 May 2002.
- [26] P. Mills, *J. Phys. Lett.* 1989, 46, 301.
- [27] P. J. Riew, P. Ghallagher, D. M. Hughes, Dispersion of subsea releases, HSE Books, Offshore Technology Report OTH 95-465, 1995.
- [28] M. Labois, D. Lakehal, *Nucl. Eng. Des.* 2011, 241, 2075.
- [29] N. A. Tsochatzidis, K. E. Maroulis, *Oil Gas J.* 2007, 105(10), 52.
- [30] J. Smart, *J. Pipeline Eng.* 2007, 6(1), 5.
- [31] J. Adachi, E. Siebrits, A. Peirce, J. Desroches, *Int. J. Rock Mech. Min. Sci.* 2007, 44, 739.
- [32] C. Narayanan, M. Labois, D. Lakehal, *7th Int. Conf. on Multiphase Flow, ICMF*, 2010.
- [33] S. Laín, M. Sommerfeld, *Powder Technol.* 2008, 184, 76.
- [34] H.-M. Prasser, M. Beyer, H. Carl, D. Lucas, A. Schaffrath, P. Schütz, F.-P. Weiß, J. Zschau, *NURETH-10*, Seoul 2003, 152(1), 3.

Manuscript received September 28, 2012; revised manuscript received January 15, 2013; accepted for publication January 15, 2013.